Original Article

Possible Reparative Effect of Stromal Vascular Fraction on Parotid Gland Injury Following Streptozotocin Induced Diabetes Mellitus. Histological Study in Adult Male Rat Model

Wafaa Abd El-Azeem Abdou Boughdady[1,2], Asmaa Ahmed El-Shafei[1] and Marwa Mohamed Sabry[1]

Department of Histology, [1]Faculty of Medicine, Cairo University, Cairo, Egypt, [2]College of Medicine, Jouf University, Saudi Arabia

ABSTRACT

Introduction and Aim of Work: Diabetes mellitus (DM) adversely affects various organs, including the parotid gland. This study aimed to evaluate the effect of adipose tissue derived stromal vascular fraction (SVF) on parotid gland injury in diabetic adult male albino rat model.

Materials and Methods: Thirty two rats were divided into the following groups: donor group, group I (control), group II (untreated diabetic), rats were injected IP with a single dose of STZ (50 mg/kg) then left untreated), and group III (SVF-treated diabetic), rats were treated as group II in addition to a single IP injection of SVF at a dose of 1.5 × 106 cells/ rat on the 7th day of STZ injection). Assessment of the parotid gland weight, biochemical analysis of tissue MDA & GSH levels, RBS, salivary glucose & α-amylase levels and salivary flow rate were done. Parotid sections were stained with HE, toluidine blue, masson trichrome, PAS, and immunostaining for BCL-2 and AQP-5. Morphometric and statistical analysis was also done.

Results: Biochemical & histological results demonstrated significant improvement in SVF-treated diabetic group compared to the untreated diabetic group. SVF treatment led to reduced levels of inflammatory markers, restored antioxidant enzyme activity, and improved glucose metabolism in the parotid gland. In addition to restoration of normal histological features of most acini. However, some acini exhibited some cells with pyknotic dark nuclei & vacuolated cytoplasm and non-clear basement membranes.

Conclusion: SVF treatment mostly restored parotid gland normal histological structure in diabetic rats suggesting the potential use of SVF in mitigating diabetes-induced damage in the parotid gland.

Received: 01 June 2024, **Accepted:** 27 July 2024

Key Words: AQP-5, BCL-2, DM, parotid gland, SVF, rat.

Corresponding Author: Wafaa Abd El-Azeem Abdou Boughdady, MD, Department of Histology, Faculty of Medicine, Cairo University, Cairo, Egypt,College of medicine, Jouf University, Saudi Arabia, **Tel.**: +20 12 7207 3909, **E-mail:** gannam362@gmail.com

ISSN: 1110-0559, Vol. 48, No. 3

INTRODUCTION

Salivary glands are the main exocrine glands in the mouth that are essential for maintaining the homeostasis of the oral cavity[1]. The parotid gland; one of the major salivary glands, is responsible for secreting over 50% of the total saliva when stimulated[2].

Salivary glands and their pathophysiology have been studied in relation to various metabolic conditions, such as diabetes mellitus[1]. Diabetes mellitus is a life-long progressive metabolic disturbance originating from either insufficient insulin production (DM type I) or the body's ineffective use of insulin (DM type II). Both cases lead to persistent hyperglycemia; the primary clinical feature associated with the condition[3].

Chronic hyperglycemia associated with DM produces oxidative damage due to release of reactive oxygen species (ROS) promoting apoptosis and multiple organ damage. In addition, development of diabetes either with insulin deficiency or resistance is accompanied by metabolic disturbance of protein, carbs, and lipids[4].

Nearly every organ in the body is impacted by diabetes mellitus, including heavy damage of the oral cavity. One of the bothersome effects of diabetes mellitus in the mouth is the disturbed function of salivary glands presented clinically in the form of dry mouth. Thus, multiple complications can occur in the oral cavity such as flourishing of a lot of bacteria, alteration in the food taste, halitosis, dental caries and difficulty in swallowing, speaking, chewing. Diabetes patients' quality of life is greatly impacted by all of these issues[5].

Atrophy of the parotid gland is a common complication of DM. This was demonstrated by the gland's decreased size and weight following acini and ducts degeneration brought on by accumulated ROS. According to multiple studies, the parotid gland exhibits noticeable degenerative alterations and are more susceptible to oxidative disturbance[2].

Stromal vascular fraction (SVF) is derived from fat tissue by enzymatic digestion, it contains various cell types, such as adipose mesenchymal stem cells (ADMSCs), smooth muscle fibers, and different leucocytes[6,7].

DOI: 10.21608/ejh.2024.292854.2074

Depending on the technique used for collection and processing, the percentage of ADMSCs in SVF can range from 40 to 50%[8].

SVF simulates ADMSCs in its properties regarding immunomodulation, angiogenesis, anti-inflammatory effects. However, SVF treatment is advantageous in two points; the first is the improved therapeutic efficacy proved in comparative experimental researches that can be attributed to the diverse cellular content of SVF. The second point is that unlike ADMSCs, SVF is easier to get as it doesn't require cell separation or special culturing conditions making it a safer option overall[9,10].

Hence, SVF is considered an optimal alternative to stem cell treatment[11]. On the other hand, one of the important drawbacks of SVF clinical use is its suitability for autologous treatments only; but not for the allogenic treatments due to the presence of various cell types in its composition that can elicit immunological rejection[9].

The current study's objective was to evaluate the impact of SVF derived from adipose tissue on parotid gland injury following diabetes induction in rat by streptozotocin (STZ).

MATERIALS AND METHODS

Chemicals

- **STZ:** It was obtained in the form of powder from Sigma-Aldrich, Cairo, Egypt and prepared freshly in the biochemistry department of Cairo University's Faculty of Medicine by dissolving in citrate buffer.
- **SVF:** It was produced from adipose tissue of rats and labeled with Paul Karl Horan- 26 (PKH-26) dye (Sigma-Aldrich, Cairo, Egypt) to trace homing of SVF cells in the parotid gland. This was done at the tissue culture unit of Histology Department, Faculty of medicine, Cairo University in the following steps[10]:
    - After donor rats were sacrificed, about 20 g of fat tissue was obtained from the adipose tissue surrounding the rat kidneys.
    - The adipose tissue was cut into small pieces and washed in phosphate buffered saline (PBS) then it was digested using 0.2% collagenase I (Sigma-Aldrich, St. Louis, MO, USA) at 37 °C for 40 min with gentle shaking at 10-min intervals.
    - Then the cell suspension was centrifuged at 700 × g for 10 min at 4 °C.
    - The supernatant was discarded, and the pellet was resuspended in PBS and filtered through a 70-µm cell strainer (Corning Inc., Corning, NY, USA).
    - The suspension was then centrifuged at 700 × g for 8 min at 4 °C. The SVF pellet was resuspended in 1 mL normal saline and was ready to use.

Animals

This experimental work included 32 albino rats that were male and adult (180-200 g, 12 weeks old). Two rats were used for preparation and isolation of SVF from adipose tissue (Donor group), and the other 30 rats were involved in the experiment. Rats were kept in the Animal House of Kasr El-Aini, Faculty of Medicine, Cairo University and were cared for in compliance with protocols that were authorized by the university's Institutional Animal Care and Use Committee (CU-IACUC) (approval number [CU III F 41 23]). They were maintained in cages made of stainless steel with normal ambient conditions and unrestricted access to food and water.

Experimental design

Three groups were created from 30 rats:

Group I (Control): 10 animals that were divided equally into 2 subgroups of 5 rats each:

- Subgroup Ia: corresponding to group II; animals received an intraperitoneal (IP) injection of citrate buffer once on the 1st day of experiment.
- Subgroup Ib: corresponding to group III; the animals received the same treatment given to subgroup Ia besides an IP injection of PBS on day 7 of the experiment.

Experimental (diabetic) groups: The remaining 20 animals were induced diabetic on the 1st day of experiment by injecting each rat IP with STZ as a single dose (50 mg/kg)[2] dissolved in 1 ml of fresh sodium citrate buffer (0.1 M, pH 4.5) (Sigma-Aldrich, Cairo, Egypt). On the 7th day of STZ injection, random blood glucose (RBG) was assessed in blood samples taken from tail veins to confirm diabetes induction[11]. All rats recorded RBG more than 250 mg/dL and confirmed diabetic, then they were split into 2 groups:

Group II (Untreated diabetic, 9 rats): Diabetic rats were left untreated till sacrifice.

Group III (SVF-treated diabetic, 11 rats): Diabetic rats received a single IP injection of PKH26-labelled SVF (1.5×10^6 cells/rat) on day 7 of STZ injection[11].

Sacrifice of all animals was conducted at the completion of the sixth week of SVF injection except for two animals of group III that were sacrificed on the 3rd day of SVF injection to track homing of SVF cells in the parotid gland tissue.

Experimental procedure: The followings were measured on day 7 of STZ injection and on the last day of experiment:

1. Water intake[12]: Water ad libitum was allowed to each rat in a 250 ml container overnight for 16 hours. Accordingly, the amount of water intake / rat/day was measured as ml/day.
2. Urine output[13]: The urine output for each animal per day (ml/day) was measured using metabolic cages with no bedding connecting to a 250 ml container.

3. Salivary flow rate[14]:

The animals were fasted for 2 hours, then anesthetized by single dose of IP injection of 1 ml/kg ketamine. Then they were injected IP with Pilocarpine hydrochloride (Sigma Aldrich, Cairo, Egypt) (0.6 mg/kg) to stimulate salivation. Total amount of saliva was collected for 10 minutes in the following steps:

Dry cotton balls were weighed (1st weight) using electronic balance and kept in the mouths of rats to absorb saliva. Then the cotton balls were removed and weighed immediately (2nd weight) after 10 minutes to avoid loss of its moisture. Total salivary flow was measured in grams by subtracting the 1st weight from the 2nd weight then converted to ml. Total saliva was divided by ten to determine the saliva flow rate in milliliters per minute.

4. Salivary glucose and α-amylase levels[14]:

Glucose and α-amylase levels were measured in the collected saliva at the Biochemistry department, Faculty of Medicine, Cairo University.

5. Random blood glucose:

Rats' tail vein blood samples were taken for calculation of RBG. This was accomplished at Faculty of Medicine's Biochemistry Department, Cairo University.

Sacrifice, parotid weight & homogenates

Sacrifice of animals was carried out after completion of experiment (7 weeks), by phenobarbital IP injection at a dose 120 mg/kg[15], at the Faculty of Medicine's Histology Department, Cairo University. The parotid glands were dissected then weighed. The left parotid samples were frozen to prepare homogenates for analysis of tissue malondialdehyde (MDA) and Glutathione (GSH) level at Faculty of Medicine's Biochemistry Department, Cairo University. While right samples were processed for histological study.

Histological studies

The right parotid samples were divided into two halves; one half was processed for preparation of semithin sections (1µm thickness) while the other half was processed for preparation of paraffin blocks from which sections of 6 µm thickness were sliced & exposed to the following:

I- Fluorescent microscopic study: Random unstained sections from the two rats (belonging to group III and sacrificed on the 3rd day of SVF injection) were examined with immunofluorescent microscope to track homing of SVF cells in glandular tissue.

II-Light microscopic study:

a. H&E stain[16].

b. Toluidine blue staining[17] (for semithin sections).

c. Masson Trichrome stain[18].

d. PAS stain[19].

e. Immunohistochemical staining[18] for:

1. Bcl-2: is a rabbit monoclonal antibody (ab 196495, abcam, USA). It is an anti-apoptotic marker that appeared as brown cytoplasmic reaction in the acinar cells.
2. Aquaporin-5 (AQP-5): is a rabbit polyclonal antibody (ab 315855, abcam, USA). It is a water channel marker that appeared as brown apical membranous reaction in the acinar cells.

For immunostaining, avidin-biotin technique was used as follows[18]:

- Antigen retrieval of the sections was done by their boiling in 10 mM citrate buffer (Cat. No, AP 9003) with a pH of 6 for 10 minutes.
- Sections were then allowed to cool at room temperature for 20 minutes.
- Sections were incubated with the primary antibodies for one hour.
- Then, immunostaining was completed using Ultravision Detection System (Cat. No, TP-015-HD) and Mayer's hematoxylin stain (Cat. No, TA-125-MH) that was used to counterstain the sections. The used materials were obtained from Lab Vision Thermo Scientific, California, USA.
- Preparation of the negative control sections was done in the same steps with omission of the primary antibodies.

Citrate buffer, Ultravision Detection System and Ultravision Mayer's hematoxylin were purchased from Labvision, ThermoFisher scientific, USA.

Positive and negative control of immunostaining

- BCL-2 positive cells showed brown cytoplasmic reaction in human colon carcinoma tissue.
- AQP-5 positive cells showed brown apical membranous reaction in rat salivary gland tissue.
- •Negative control of BCL-2 and AQP-5 showed negative immunostaining in rat parotid gland tissue (Figure 1).

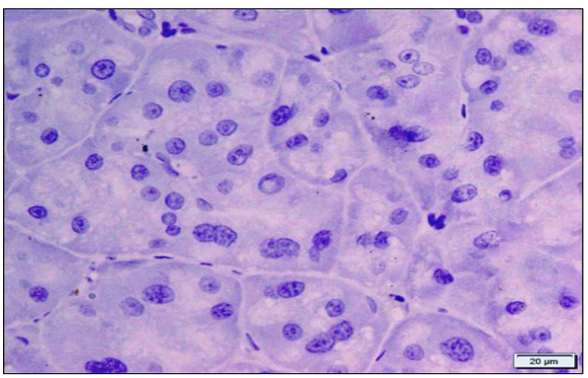

Fig. 1: Photomicrograph of a section of rat parotid gland illustrating negative immunostaining. (Negative control of immunostaining X400).

Morphometric study

Image analysis was performed using Leica Qwin 500 C" image analyzer computer system (Cambridge, England) at Histology Department, Faculty of Medicine, Cairo University. Area percent of collagen fibers, PAS +ve reaction, bcl-2 and AQP-5 +ve immunoreactivity was calculated in the related sections in 10 fields without overlap from different sections belonging to each group separately (×400).

Statistical analysis

It was done for morphometric and biochemical findings using SPSS software (version 21) and presented as mean ± standard deviation (SD). To do comparison between various groups, ANOVA test was employed, then a post hoc Tukey test was done. Statistical significance was determined by evaluating the p-value, and differences were deemed of statistical significance when the *p-value* was lower than 0.05[20].

RESULTS

General observations

- No rats died throughout the experiment.
- Subgroups of group I displayed comparable findings so, collectively were presented as the control group.
- All rats in the experimental group experienced diabetes with the typical symptoms of polydipsia and polyuria.

Water intake & urine output

They showed significant increase in groups II & III versus the control group. But group II revealed significant increase in comparison with group III (Histogram 1a, Table 1).

Parotid weight

It was markedly decreased in group II in contrast to group I and III with a non-significant difference between group I and III (Histogram 1b, Table 2).

Tissue MDA & GSH levels

MDA level revealed significant elevation & GSH level demonstrated significant descent in both group II & III versus group I. Nevertheless, a dramatic difference between group II & III was detected (Histogram 1b, Table 2).

RBG & salivary glucose level

Both levels showed significantly higher values in groups II and III in comparison with group I. However, a marked increase was detected in both parameters in group II versus group III (Histogram 2a, Table 3).

Salivary flow rate and α-amylase level

Both levels expressed significant reduction in group II in contrast to group I and III with a negligible difference between group I and group III (Histogram 2b, Table 4).

Histological results

H&E stained sections

Group I (Control) illustrated the typical histological structure of parotid gland, comprising lobes and lobules separated by CT septa. The parenchyma comprised densely packed pure serous acini with clear basement membranes, pyramidal serous cells exhibiting basophilic cytoplasm and rounded basal nuclei. Intralobular and excretory ducts were also seen (Figures 2a-2c).

Group II (untreated diabetic group): showed irregular lobes separated by CT septa. The serous acini were irregular, distorted with disrupted non clear basement membranes and lined by serous cells exhibiting dark, pyknotic & pleomorphic nuclei and highly vacuolated cytoplasm. Heavy inflammatory infiltration around excretory ducts and congested blood vessels were also seen. (Figures 3a-3c).

Group III (SVF-treated diabetic group): revealed apparently normal lobes separated by CT septa and histological restoration of the normal structure of most of the parotid acini. However, some acini showed non clear basement membranes and some serous cells with pyknotic dark nuclei and cytoplasmic vacuolations. Normal ducts were also seen (Figures 4a,4b).

Semithin stained sections

Group I showed normal serous acini with a lining of pyramidal serous cells with vesicular nuclei and clear nucleoli. Their cytoplasm revealed apical uniform dense secretory granules. Myoepithelial cells with flat nuclei were detected surrounding the intact clear basement membrane of serous acini. Group II showed distorted acini with disrupted basement membranes & lined by serous cells having pyknotic dark nuclei or irregular shrunken dark nuclei and vacuolated cytoplasm. Group III appeared with almost normal architecture. The serous acini appeared normal except for some serous cells exhibited pyknotic darkened nuclei and cytoplasmic vacuolations (Figures 5a-5c).

Masson trichrome stained sections

Showed mild collagen fiber deposition in group I and moderate collagen deposition in group III while group II showed heavy deposition of collagen fibers (Figures 6a-6c).

PAS stained sections

Showed strong +ve cytoplasmic PAS reaction in the serous cells in both group I and III while group II showed weak reaction (Figures 7a-7c).

BCL2 immunostained sections

Showed strong positive immunoreaction for BCL2 in the cytoplasm of acinar cells in both group I and III while group II showed weak reaction (Figures 8a-8c).

AQP-5 immunostained sections

Showed strong membranous positive immunostaining in the apical cell membranes in almost all acinar cells in both group I and III and weak reaction in group II (Figures 9a-9cd).

Detection of PKH26 labelled SVF cells with fluorescent microscope in unstained parotid sections of group III

Illustrated red fluorescence of multiple PKH26 labelled SVF cells within the parotid interstitium (Figure 10).

Morphometric results

Area percent of collagen fibers was significantly increased while area percent of PAS, BCL2 and AQP-5 positive reaction was markedly decreased in group II & III relative to group I. But group III demonstrated significant improvement in all these parameters versus group II (Histogram 3, Table 5).

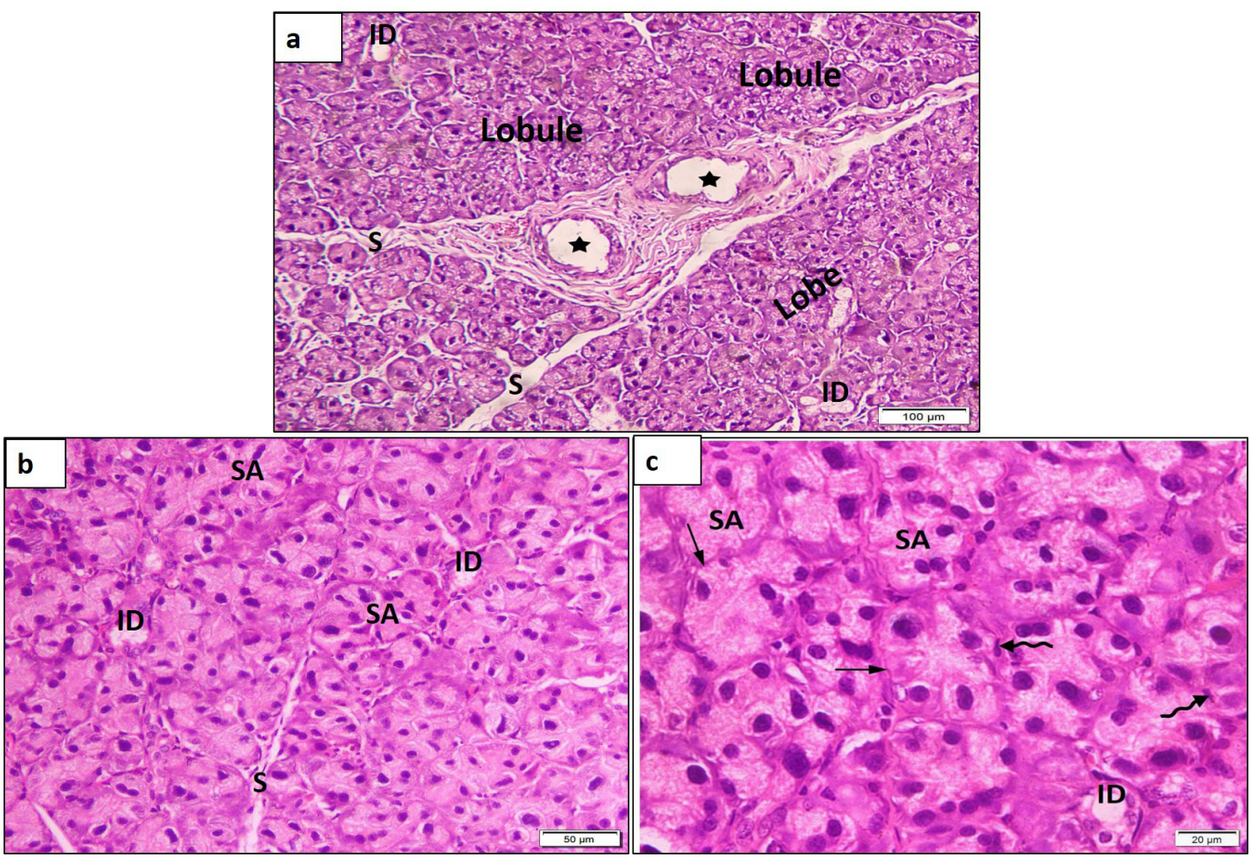

Fig. 2: Photomicrographs of parotid sections of group I showing: a: Parotid lobules (Lobule) and lobes (Lobe), separated by CT septa (S), intralobular ducts (ID) and Excretory ducts (star) [x100]. b: The lobules are formed of closely packed rounded purely serous acini (SA) & intralobular ducts (ID). Note connective tissue septa (S) between lobules [x200]. c: The serous Acini (SA) have pyramidal cells with basophilic cytoplasm, rounded basal nuclei and surrounded by clear basement membranes (arrows). Note myoepithelial cells with flat nuclei (wavy arrow) and intralobular ducts (ID) [x400].

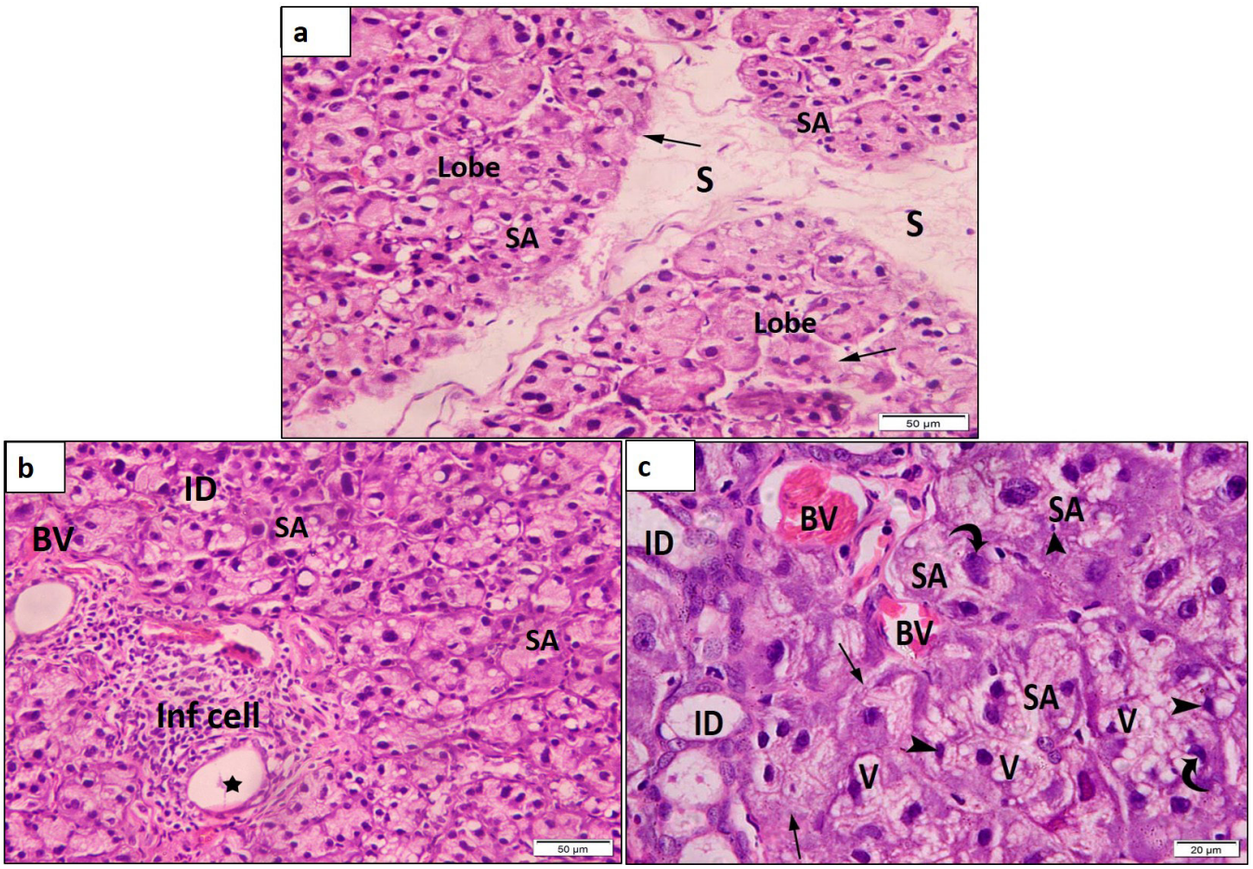

Fig. 3: Photomicrographs of parotid sections of group II illustrating: a: irregular lobes (Lobe) separated by CT septa (S), irregular distorted serous acini (SA) with disrupted non clear basement membranes (arrows) [x200]. b: demonstrating congested blood vessels and heavy inflammatory cellular infiltration (Inf cell) around excretory ducts (star). Note distorted serous acini (SA) and intercalated ducts (ID) [x200]. c: showing serous acini (SA), lined by cells with pyknotic dark (arrowheads) & pleomorphic nuclei (curved arrows) and highly vacuolated cytoplasm (V). Note intercalated ducts (ID) and congested blood vessels (B.V) [x400].

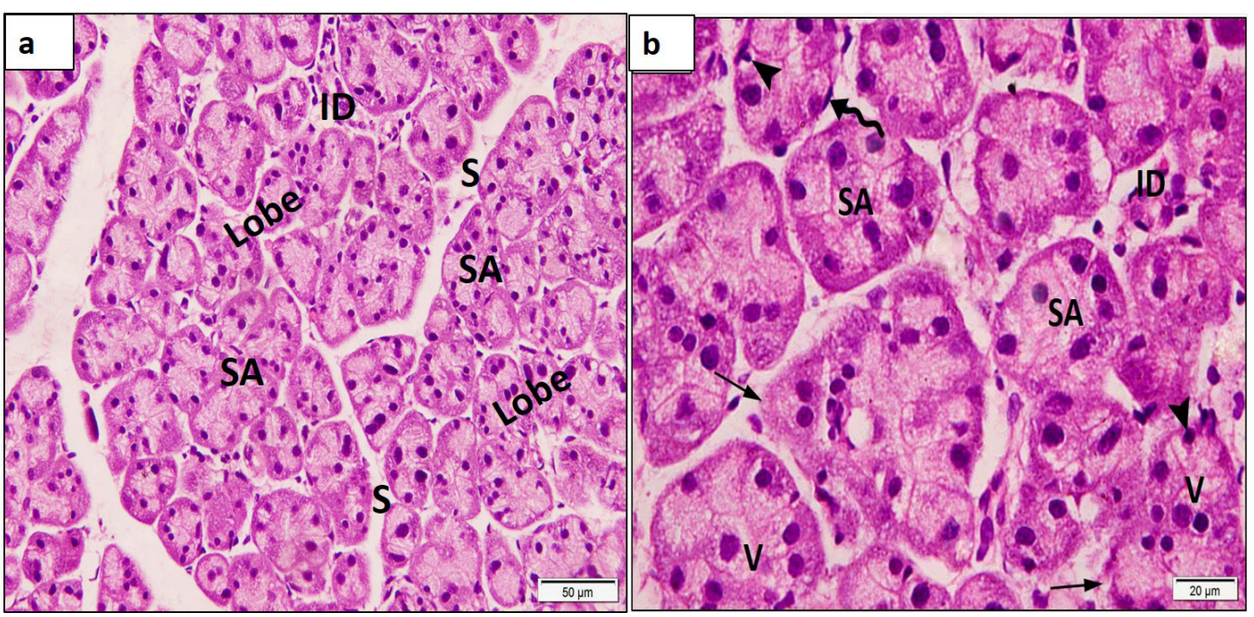

Fig. 4: Photomicrographs of group III revealing: a: apparently normal lobes (lobe), separated by CT septa (S), normal serous acini (SA) and intralobular ducts (ID) [x200]. b: Some serous acini display non clear basement membranes (arrows) and some cells having pyknotic dark nuclei (arrowheads) and cytoplasmic vacuolation (V). Note myoepithelial cells with flat nuclei (wavy arrow) surrounding the acini [x400].

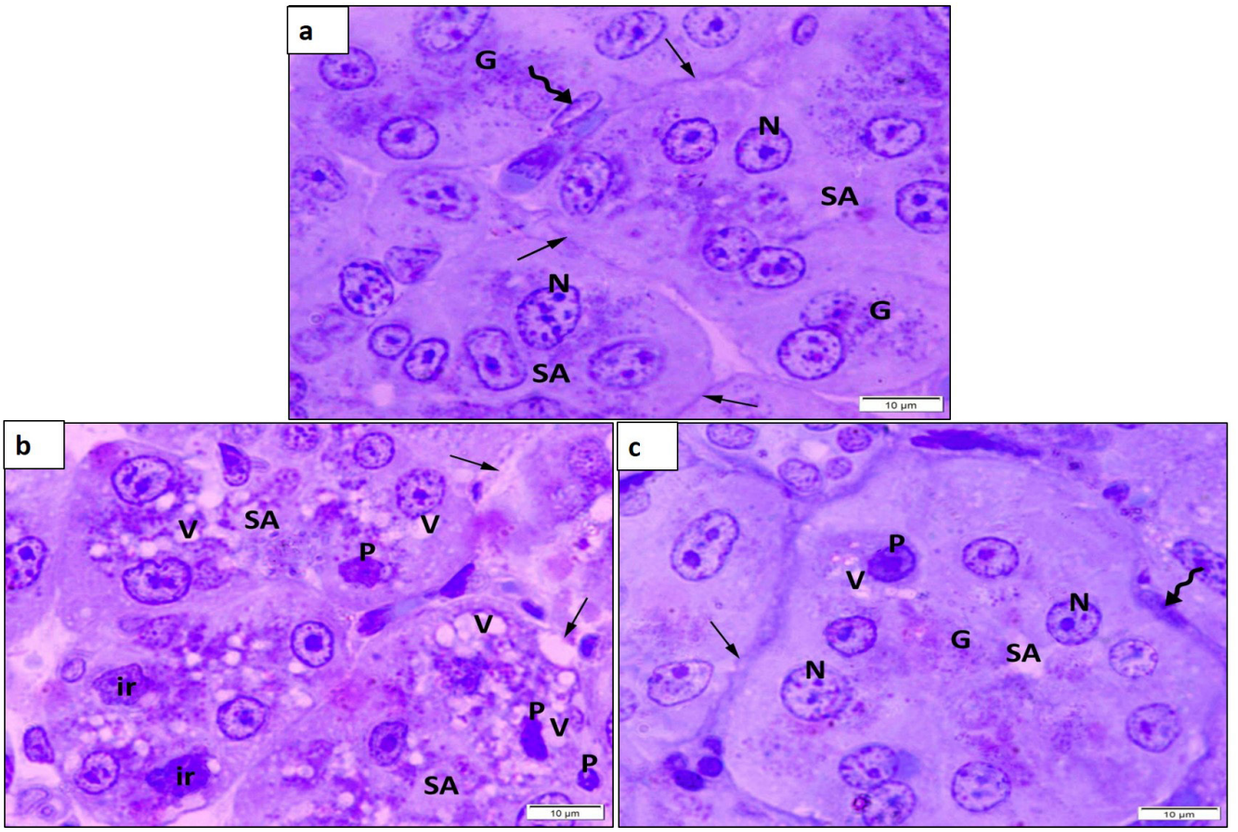

Fig. 5: Photomicrographs of toluidine blue stained semithin parotid sections: a: group I: illustrating normal serous acini (SA) with intact clear basement membranes (arrows). They are lined by pyramidal serous cells showing vesicular nuclei (N) with clear nucleoli & apical uniform dense secretory granules (G). Note myoid cells with flat nuclei (wavy arrow) surrounding serous cells [x1000]. b: group II: showing distorted serous acini (SA) and serous cells with pyknotic dark nuclei (P), irregular shrunken dark nuclei (ir) and multiple cytoplasmic vacuoles (V). Note disrupted basement membranes (arrow) [x1000]. c: group III: revealing apparently normal serous acini (SA) with intact clear basement membranes (arrows) surrounded by myoid cells with flat nuclei (wavy arrow). The acini are lined by pyramidal serous cells exhibiting vesicular nuclei (N) with clear nucleoli & apical uniform dense secretory granules (G). Note a serous cell with dark pyknotic nucleus (P) and cytoplasmic vacuoles (V) [x1000].

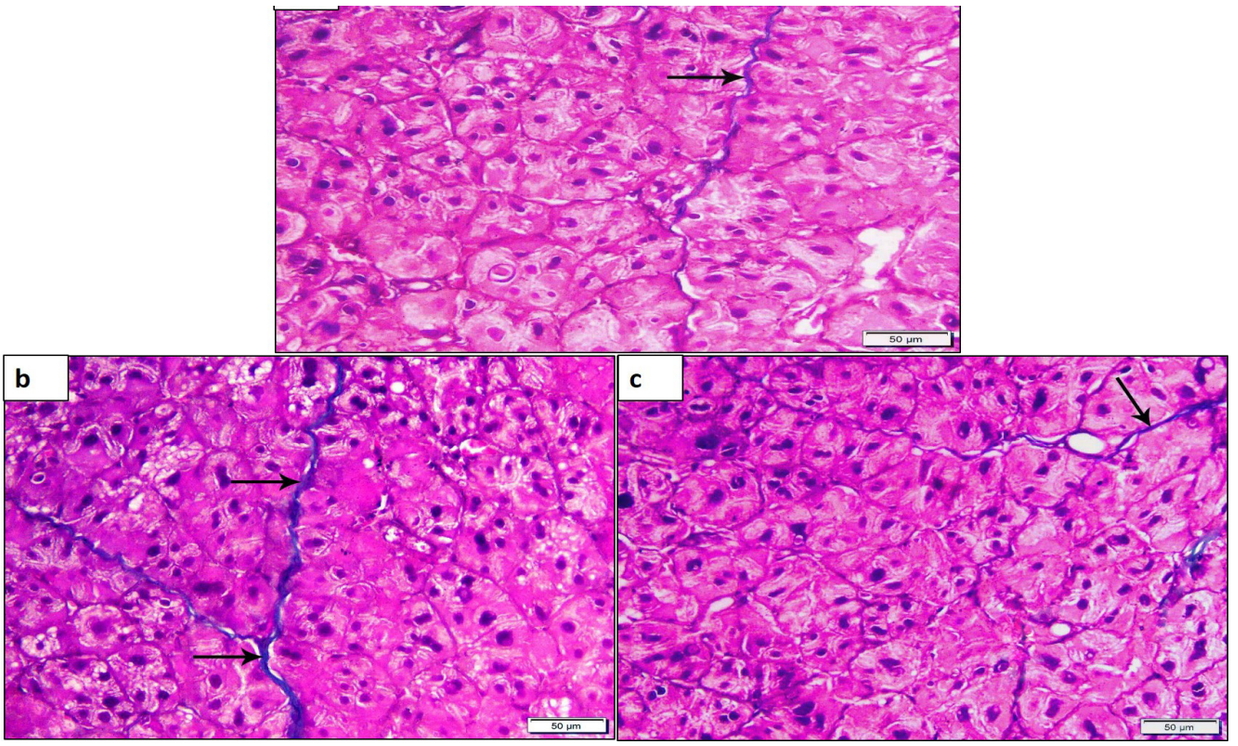

Fig. 6: Photomicrographs of masson trichrome sections: a: group I: demonstrating mild collagen fiber deposition (arrow). b: group II: displaying heavy collagen fiber deposition (arrows). c: group III: illustrating moderate collagen fiber deposition [x200].

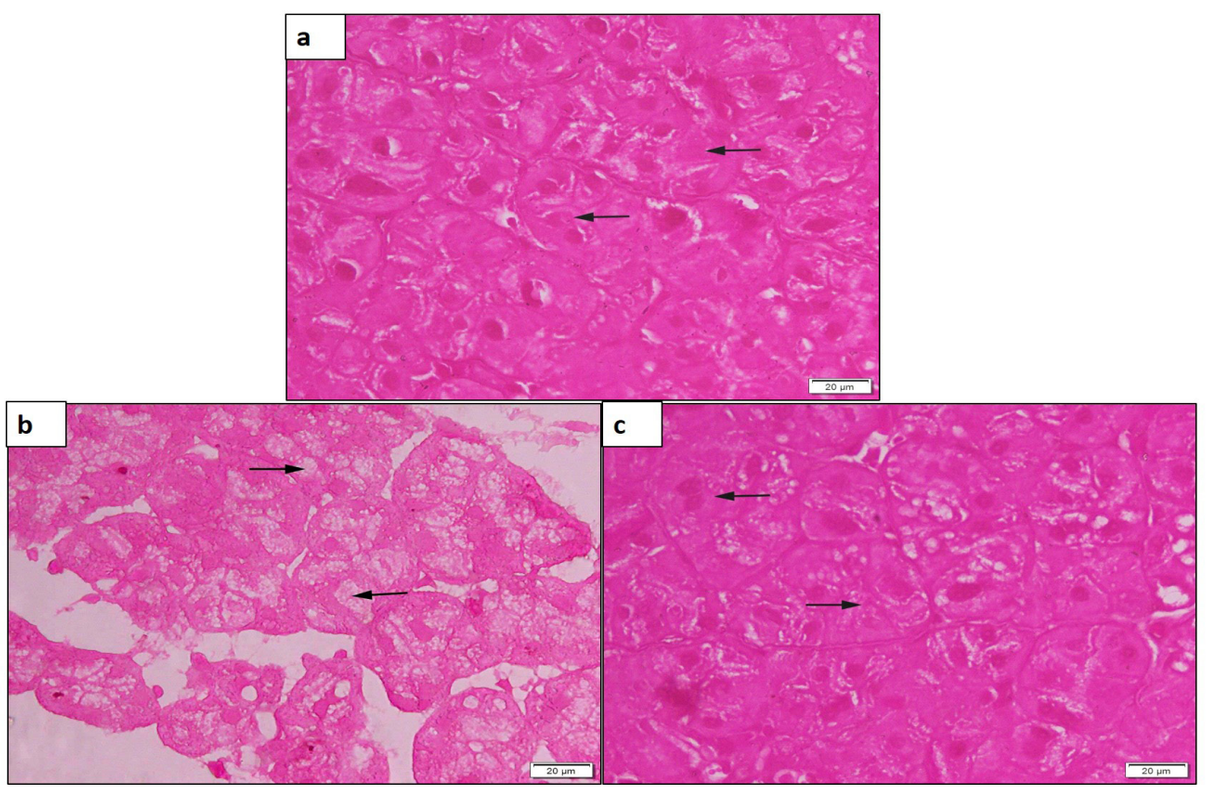

Fig. 7: Photomicrographs of PAS stain: a: group I & c: group III: displaying strong +ve cytoplasmic PAS reaction (arrows) in the serous cells while b: group II: displaying mild reaction (arrows) in the serous cells [x400].

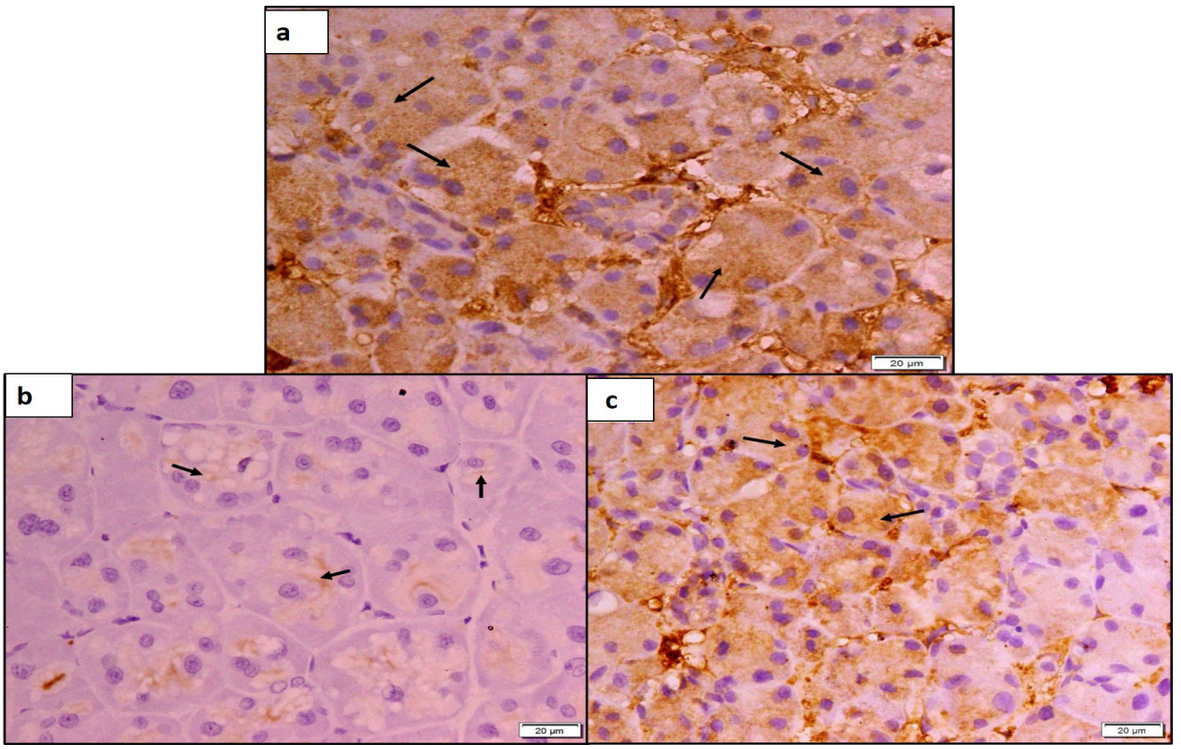

Fig. 8: Photomicrographs of BCL2 immuno-staining: a: group I & c: group III: revealing: strong +ve cytoplasmic reaction in the acinar cells (arrows). b: group II: illustrating weak reaction (arrows) [x400].

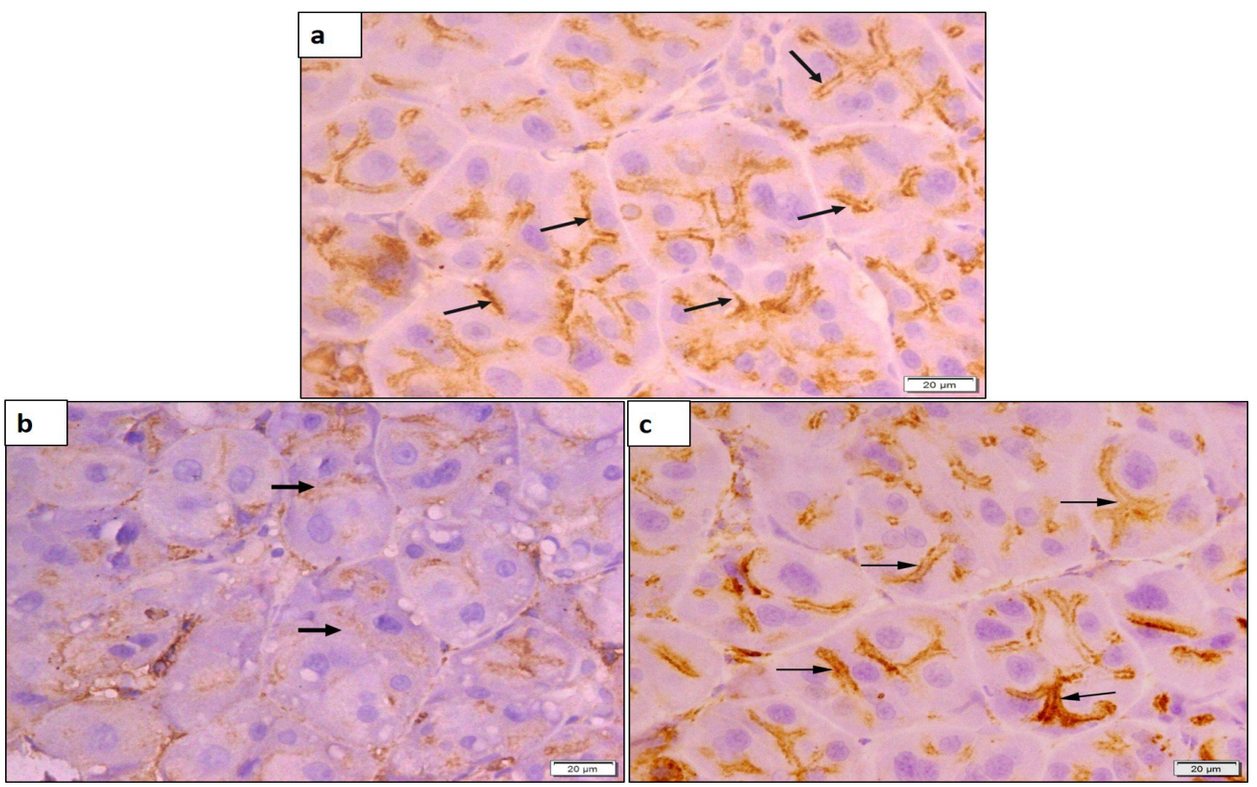

Fig. 9: Photomicrographs of AQP-5 immuno-staining: a: group I & c: group III: revealing strong membranous +ve immunostaining in the apical cell membranes (arrows) in almost all acinar cells. b: group II: showing weak reaction (arrows) [x400].

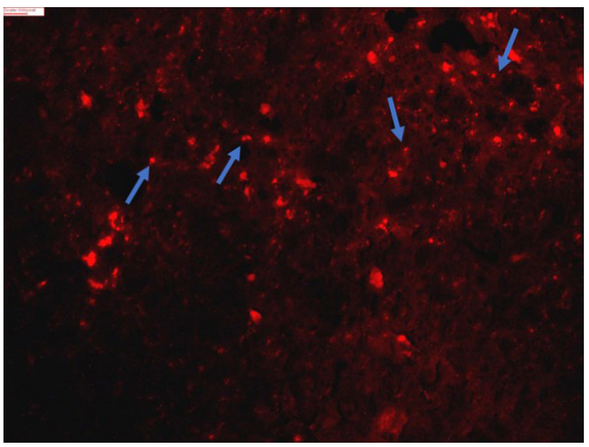

Fig. 10: Fluorescent micrograph of unstained parotid sections of group III showing red fluorescence of multiple PKH-26 labelled SVF cells within the parotid interstitium (arrows) [PKH26 fluorescent dye, X 200].

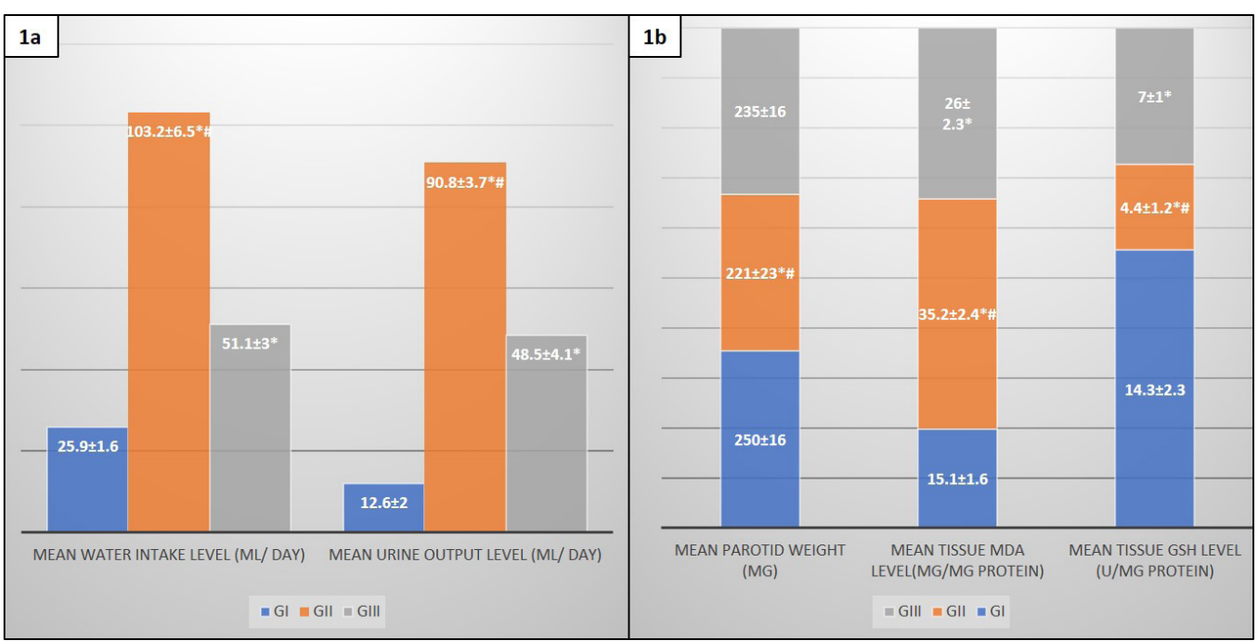

Histogram 1: showing a: Mean water intake & urine output level in all groups (ml/ day). b: Mean level of parotid weight & tissue MDA & GSH in all groups. *Significant regarding group I. # Significant regarding group III.

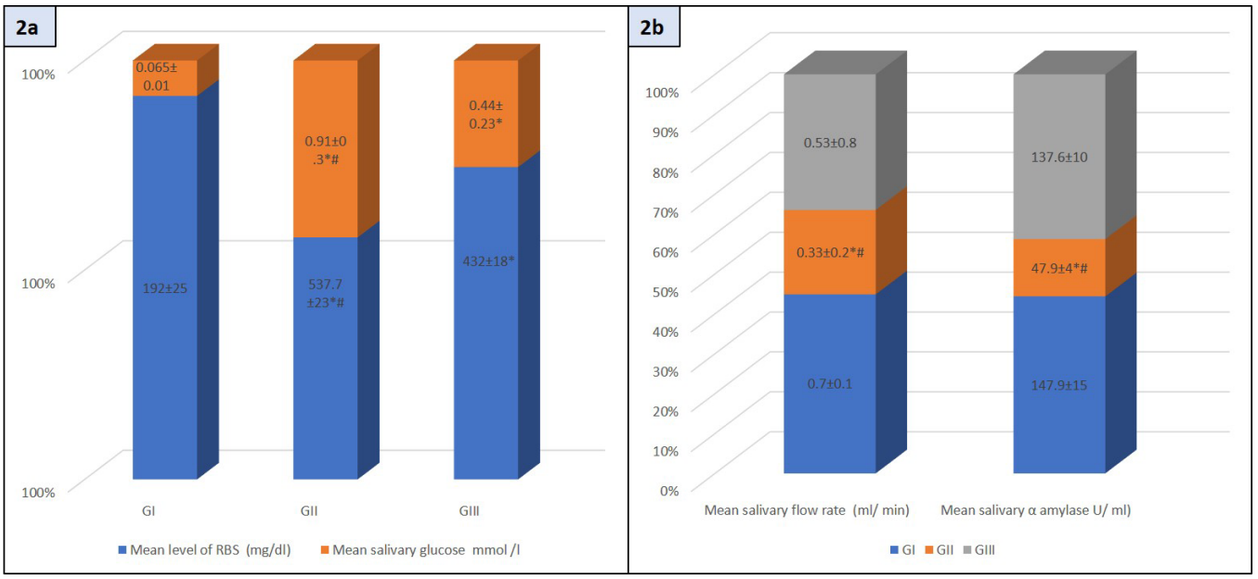

Histogram 2: demonstrating: a: mean level of RBS & salivary glucose, b: salivary flow rate & salivary α amylase in all groups.
*Significant regarding group I. # Significant regarding group III.

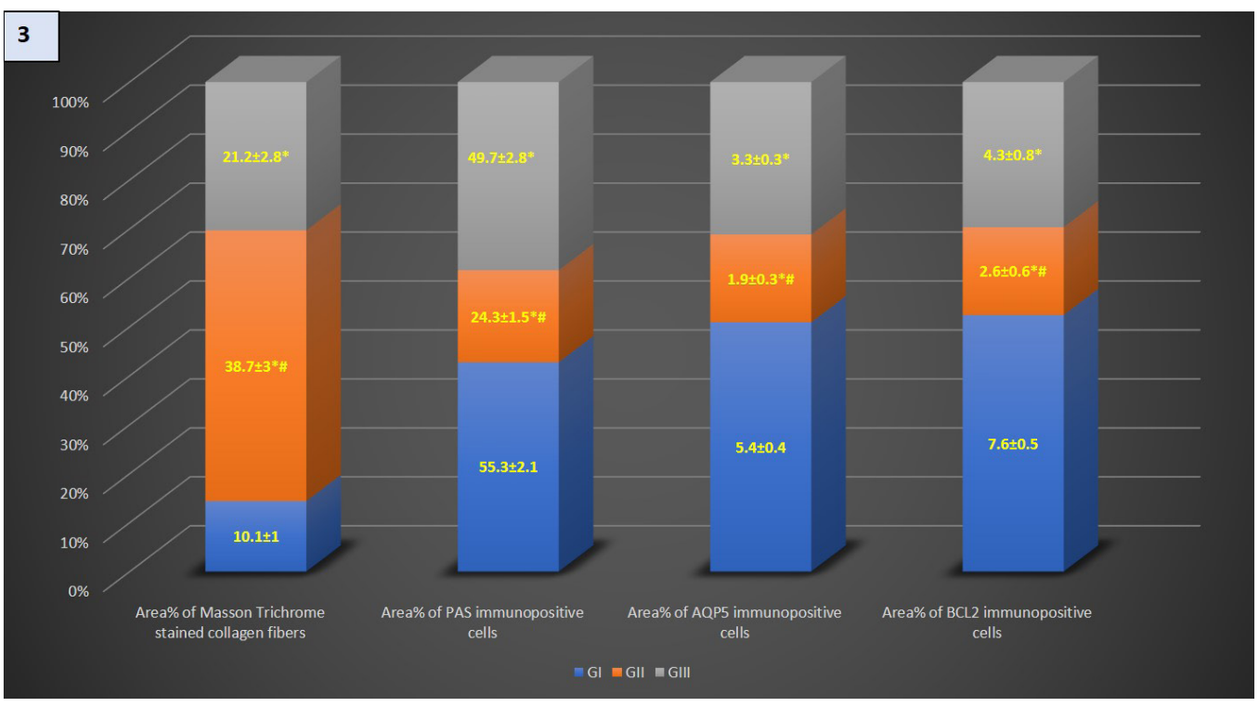

Histogram 3: showing mean area % of collagen fibers & PAS, AQP5, BCL2 positive reactivity in all groups.
*Significant regarding group I. # Significant regarding group III.

Table 1: Mean water intake & urine output level in all groups (ml/ day)

Groups	Mean water intake level (ml/ day)	Mean urine output level (ml/ day)
GI	25.9±1.6	12.6±2
GII	103.2± 6.5*#	90.8±3.7*#
GIII	51.1±3*	48.5±4.1*

*Significant regarding group I.
Significant regarding group III.

Table 2: Mean level of parotid weight, tissue MDA & GSH in all groups

Groups	Mean parotid weight (mg)	Mean tissue MDA level (µg/mg protein)	Mean tissue GSH level (u/mg protein)
GI	250±16.7	15.1±1.6	14.3±2.3
GII	221±23*#	35.2± 2.4*#	4.4±1.2*#
GIII	235±16	26±2.3*	7±1*

*Significant regarding group I.
Significant regarding group III.

Table 3: Mean level of RBG & salivary glucose in all groups

Groups	Mean level of RBG (mg/dl)	Mean salivary glucose mmol /l
GI	192±25	0.065±0.01
GII	537.7± 23*#	0.91±.0.3*#
GIII	432.3±18*	0.44±0.23*

*Significant regarding group I.
Significant regarding group III.

Table 4: Mean level of salivary flow rate & salivary α amylase in all groups

Group	Mean salivary flow rate (ml/ min)	Mean salivary α amylase U/ ml)
GI	0.7±0.1	147.9±15
GII	0.33± 0.2*#	47.9± 4*#
GIII	0.53±0.8	137.6±10

*Significant regarding group I.
Significant regarding group III.

Table 5: Mean area% of collagen fibers, PAS, AQP5 & BCL2 positive reaction in all groups

Group	Area % of collagen fibers	Area% of PAS positive reaction	Area% of positive AQP5 immunoreactivity	Area% of positive BCL2 immunoreactivity
GI	10.1±1	55.3±2.1	5.4±0.49	7.6±0.56
GII	38.7±3*#	24.3±1.5*#	1.9±0.32*#	2.6±0.62*#
GIII	21.2±2.8*	49.7±2.8*	3.3±0.32*	4.3±0.81*

*Significant regarding group I.
Significant regarding group III.

DISCUSSION

Diabetes mellitus was proven to have detrimental effects on the parotid gland, resulting in reduced salivary flow and changes in saliva composition, increasing the risk of oral health issues[21]. The objective of this work was to assess the impact of fat tissue- derived SVF on injury of parotid gland following diabetes induction in rat by STZ.

The observation of polydipsia and polyuria in the diabetic rats (group II and III) is in line with clinical manifestations seen in human diabetes, further validating the relevance of the rat model for studying diabetes-related changes. These symptoms are indicative of altered water and electrolyte homeostasis resulting from the metabolic abnormalities associated with diabetes[22].

The parotid gland weight demonstrated significant decline in group II (untreated diabetic) relative to the control group suggesting structural changes or atrophy associated with diabetes, which was improved in group III (SVF-treated diabetic). These findings were concomitant with a previous study that reported reduction in weight and size of the gland, due to degeneration of acinar cells and intralobular ducts by accumulated ROS in a diabetic rat model[2].

In the current study, the increased tissue malondialdehyde (MDA) level in group II and III signify heightened oxidative stress in the diabetic condition, potentially contributing to parotid gland dysfunction[23]. Concurrently, the decreased tissue glutathione (GSH) level in group II and III indicated compromised antioxidant defenses[24]; however, there was a notable difference between the SVF-treated and untreated diabetic groups.

In addition, this study revealed a marked reduction in salivary glucose level in group III versus group II. Furthermore, salivary flow rate and α-amylase levels declined significantly in group II compared to both group I and III. These findings could be explained by chronic hyperglycemia and oxidative stress that can lead to cellular injury and dysfunction of the cells in the gland acini. This can result in reduced synthesis and secretion of salivary components, including α-amylase, an enzyme responsible for the breakdown of starches into simpler sugars[25].

In H&E & semithin sections, the untreated diabetic group (II), exhibited significant histological alterations in the parotid gland including irregular acini, disrupted non clear basement membranes, dark pyknotic & pleomorphic nuclei, cytoplasmic vacuolation of the acinar cells, inflammatory cellular infiltration, and congested blood vessels. These changes were confirmed by a previous study[26] which found that parotid gland of diabetic rats displayed parenchymal atrophy presented in form of disruption of gland architecture, damaged acini, and dilated ducts. Identical observations were recorded by previous authors who related the nuclear and cytoplasmic changes to hyperglycemia promoting release of free radicals associated with oxidative stress and leading to cellular apoptosis and degeneration[4].

These findings could be explained by microvascular changes associated with diabetes as parotid gland receives its blood supply from various arteries. Diabetic microangiopathy, a condition involving damage to small blood vessels, may affect the blood flow to the gland, leading to histopathological changes. In addition, diabetes is associated with increased oxidative stress, which can lead to cellular damage[27].

Interestingly, the SVF-treated diabetic group (III) demonstrated a restoration of the normal histological features in most of the acini, with clear and intact basement membranes. However, some serous cells with pyknotic dark nuclei and cytoplasmic vacuolations were noted in some acini exhibiting non clear basement membranes. This could suggest that the SVF treatment had an ameliorative effect on the histological architecture of the parotid gland, promoting the regeneration or preservation of acinar structures.

The mechanism of action of SVF is thought to be primarily mediated by their content of adipose mesenchymal stem cells (ADMSCs) which represent 40-50% of the cell population. The regenerative potential of ADMSCs lies in their ability to contribute to tissue repair and regeneration by generating new cells to replace damaged or lost tissue[28]. Additionally, they secrete bioactive molecules, including growth factors and cytokines, with paracrine effects such as promoting angiogenesis and recruiting cells involved in tissue repair[29].

Moreover, ADMSCs exhibit immunomodulatory properties, suppressing inflammatory responses and regulating immune cell activity, which can be advantageous in conditions involving excessive inflammation or autoimmune responses[30]. Furthermore, ADMSCs contribute to extracellular matrix (ECM) remodeling, releasing enzymes and proteins that degrade and reconstruct the ECM. Their interactions with local microenvironment cells, including resident stem cells and tissue-specific cells, influence neighboring cell behavior, fostering tissue regeneration and repair[31].

In the current study, masson trichrome staining revealed marked collagen deposition in group II, indicating presence of fibrotic changes which were confirmed by a significant elevation in area % of collagen fibers in group II in comparison with the control group (I) and SVF treated diabetic group (III). Fibrosis is often accompanied by chronic inflammation and tissue damage, and its increase in the untreated diabetic group underscores the severity of parotid gland alterations[32]. These changes were in line with a previous research that recorded marked collagen deposition and increased fibrosis in the diabetic mice parotid gland relative to the control mice. The fibrotic changes were accompanied by chronic inflammation, further confirmed by elevated levels of pro-inflammatory markers detected through immunohistochemical analysis[33].

In contrast, the SVF-treated diabetic group showed moderate collagen fiber deposition, suggesting a potential

mitigating effect of SVF on fibrosis. In line with our results, a pervious study found that the radiation-induced salivary gland injury group exhibited significant fibrosis with marked collagen deposition. However, in rats with radiation-induced salivary gland injury & treated with SVF, there was a notable reduction in collagen fiber deposition, suggesting a mitigating effect of SVF on fibrosis[34].

The mitigating effect of SVF on fibrosis might be related to the ability of SVF to decrease the expression of certain cytokines and inflammatory mediators such as transforming growth factor- β1 (TGF-β1), which is an important profibrogenic inducer. On the other hand, SVF might induce the expression of important anti-fibrotic mediators such as TGF-β3 and hepatocyte growth factor (HGF). Previous studies on different organs supported this suggestion[35,36].

Regarding PAS stained sections of this study, the untreated diabetic group exhibited a mild cytoplasmic reaction in the acinar cells, suggesting a reduction in their glycoprotein content. Such results were confirmed by significantly decreased area percent of PAS +ve reaction in group II when compared to group I and III. In harmony with our results. Another study mentioned that diabetic patients with periodontal disease showed a mild reaction with PAS staining[1]. In the same concern, other authors explained that saliva, rich in glycoproteins, helps to preserve the mouth by lubricating and masking the teeth and oral tissues, preventing bacterial adhesion and promoting oral health. They added that reduction in glycoprotein content observed in the diabetic group may compromise the protective and lubricating properties of saliva[37].

On the other hand, a strong positive PAS reaction was recorded in the SVF-treated diabetic group in this study, indicating availability of glycoproteins in the secretory structures. This suggests that SVF treatment may have a positive effect on the glycoprotein content in the parotid glands. This finding can have important implications for oral health. SVF treatment may promote tissue regeneration and modulate the inflammatory response, which can potentially affect the production and secretion of glycoproteins[38].

BCL2 is an anti-apoptotic protein that performs a central role in maintaining cell viability and preventing apoptosis or programmed cell death[39]. In present study, immunostaining for BCL2 revealed a weak reaction in the untreated diabetic group confirmed by significantly decreased area percent of BCL2 +ve immunoreactivity versus group I and III. This was concomitant with a study that found a weak reaction in the sections of diabetic rats, indicating decline in BCL2 expression. Apoptosis is an essential cellular process involved in tissue homeostasis, and dysregulation of apoptosis can result in tissue damage and dysfunction[2]. In the context of diabetes, sustained hyperglycemia and oxidative load can lead to the activation of apoptotic pathways and an imbalance between cell survival and death[40].

While BCL2 sections of the SVF-treated diabetic group illustrated a strong positive reaction suggesting that SVF treatment might potentially preserve BCL2 expression and protect against apoptosis. This could be due to the presence of various cell types within SVF, as adipose stem cells and immune cells, which can secrete factors that promote cell survival and modulate apoptotic pathways[41].

Aquaporins are a protein family playing a crucial task in facilitating the movement of water across cell membranes. AQP-5, specifically, is expressed in different tissues, including the salivary glands, lungs, and kidney, where it contributes to the regulation of water transport[42]. AQP-5 immunostaining in the current work revealed a significant descent in area percent of AQP-5 +ve immunopositivity in the untreated diabetic group in contrast with group I and III. In agreement with a study previously reported a decreased AQP-5 protein expression in membranes of acinar cells in sections of diabetic rats compared to control rats[43]. Hyperglycemia and altered metabolic pathways associated with diabetes could impact the regulation of AQP-5 at the transcriptional or translational level. In addition, inflammatory processes and oxidative stress, intimately associated with diabetes, might also contribute to the observed changes in AQP-5 expression[44].

A strong positive AQP-5 immunostaining was noticed in group III. This implies that the SVF treatment may have a beneficial effect on the water transport mechanisms in the context of diabetes, possibly contributing to the maintenance of normal cellular functions related to water balance as it was previously proved that ADMSCs isolated from SVF transdifferentiate into acinar cells with expressed markers such as α-amylases and AQP-5[45].

Morphometric analysis further quantified the previously mentioned histological results with significant elevation in area percentage of PAS, BCL2, and AQP-5 +ve reaction in group III relative to group II. This highlights the impact of SVF on the preservation of glycoprotein content, protection against apoptosis, and regulation of water transport function. Moreover, the observation of PKH26-labeled SVF cells within the parotid interstitium of group III confirms the integration of SVF cells into the tissue, supporting the notion that SVF treatment may contribute to the observed histological restoration.

CONCLUSION

The histological and immunohistochemical findings in this study collectively suggest that diabetes could induce profound structural and molecular alterations in the parotid glands, including inflammation, fibrosis, changes in glycoprotein content, apoptosis, and alterations in water transport function. On the other hand, SVF treatment demonstrated a potential therapeutic effect by mitigating these alterations, preserving normal glandular architecture, and influencing various molecular pathways. However, further researches are recommended to fully elucidate the underlying mechanisms and therapeutic potential of SVF use in diabetic induced parotid gland injury.

CONFLICT OF INTERESTS

There are no conflicts of interest.

REFERENCES

1. Fouani M, Basset CA, Jurjus AR, Leone LG, Tomasello G and Leone A. Salivary gland proteins alterations in the diabetic milieu. Journal of Molecular Histology. 2021; 52: 893-904. doi:10.1007/s10735-021-09999-5.
2. Al Serwi RH, El Kersh AOF and El Akabawy G: Human dental pulp stem cells attenuate streptozotocin induced parotid gland injury in Rats. Stem Cell Research &Therapy. 2021; 12: 577. doi: 10.1186/s13287-021-02646-6.
3. Yasser S and Shon AA: Histomorphometric and Immunohistochemical Study Comparing Submandibular Salivary Glands of Albino Rats. Maced J Med Sci. 2020; 8: 49-54. https://doi.org/10.3889/oamjms.2020.3722.
4. El-Ghazawy YM, El-Zainy MA and Hassan R: Histological and Immunohistochemical Analysis of Green Coffee Aqueous Extract Effect on Parotid Salivary Gland in Streptozotocin Induced Diabetic Albino Rats. EJH. 2020; 43: 748-762. DOI: 10.21608/EJH.2019.20725.1211.
5. Narmada IB, Laksono V, Nugraha AP, Ernawati DS, Winias S, Prahasanti C, Dinaryanti A, Susilowati H, Hendrianto E, Ihsan IS and Rantam FA: Regeneration of Salivary Gland Defects of Diabetic Wistar Rats Post Human Dental Pulp Stem Cells Intraglandular Transplantation on Acinar Cell Vacuolization and Interleukin-10 Serum Level. Pesqui. Bras. Odontopediatria Clín. Integr. 2019; 19: e5002. https://doi.org/10.4034/PBOCI.2019.191.144.
6. Karatan B, Akşam E, Erden E and Demirseren ME: Effects of adipose derived stromal vascular fraction on diabetic neuropathy: an experimental study. Journal of Plastic Surgery and Hand Surgery. 2019; 53: 335-340. doi: 10.1080/2000656X.2019.1632205.
7. Quaade ML, Dhumale P, Steffensen SG, Beck HC, Harvald EB, Jensen CH, Lund L, Andersen DC and Sheikh SP: Adipose-Derived Stem Cells from Type 2 Diabetic Rats Retain Positive Effects in a Rat Model of Erectile Dysfunction. Int. J. Mol. Sci. 2022; 23: 1692. doi: 10.3390/ijms23031692.
8. Farid MF, Abouelela YS, Yasin NAE, Al Mokaddem AK, Prince A, Ibrahim MA and Rizk H: Laser-activated autologous adipose tissue-derived stromal vascular fraction restores spinal cord architecture and function in multiple sclerosis cat model. Stem Cell Research & Therapy. 2023; 14: 6. https://doi.org/10.1186/s13287-022-03222-2.
9. Bora P and Majumdar AS: Adipose tissue-derived stromal vascular fraction in regenerative medicine: a brief review on biology and translation. Stem Cell Research & Therapy. 2017; 8: 145. doi: 10.1186/s13287-017-0598-y.
10. Yang WT, Ke CY, Yeh KT, Huang SG, Lin ZY,Wu WT and Lee RP: Stromal vascular fraction and adipose derived stem cell therapies improve cartilage regeneration in osteoarthritis induced rats. Scientific reports. 2022; 12: 2828. doi: 10.1038/s41598-022-06892-3.
11. Sayed SY, Salem SI, Abdallah AN, Khalil GM and Mohammed FF: Clinicopathological studies on the use of laser-activated adipose-derived stromal vascular fraction in treatment of streptozotocin-induced diabetes in rats. Comp Clin Pathol. 2019; 28:1515-152. DOI:10.1007/s00580-019-03008-8.
12. Stewart CR, Obi N, Epane EC, Akba AA, Halpern L, Southerland JH and Gangula PR: The Effects of Diabetes on Salivary Gland Protein Expression of Tetrahydrobiopterin and Nitric Oxide Synthesis and Function. J Periodontol. 2016; 87: 735-41. doi: 10.1902/jop.2016.150639.
13. Turner T, Chen X, Zahner M, Opsahl A, DeMarco G, Boucher M, Goodwin B and Perreault M: FGF21 increases water intake, urine output and blood pressure in rats. PLoS ONE. 2018; 13: e0202182. doi: 10.1371/journal.pone.0202182.
14. Bhattarai KR, Lee HY, Kim SH, Kim HR and Chae HJ: Ixeris dentata Extract Increases Salivary Secretion through the Regulation of Endoplasmic Reticulum Stress in a Diabetes-Induced Xerostomia Rat Model. Int J Mol Sci. 2018; 19:1059. doi: 10.3390/ijms19041059.
15. Pourghasem M, Nasiri E and Shafi H: Early renal histological changes in alloxan-induced diabetic rats. Int J Mol Cell Med. 2014; 3: 11-5. doi: PMID: 24551816; PMCID: PMC3927393.
16. Kuru K: Optimization and enhancement of H and E stained microscopical images by applying bilinear interpolation method on lab color mode. Theoretical Biology and Medical Modelling. 2014; 11:9-18. doi: 10.1186/1742-4682-11-9.
17. Hayat MA: Chemical fixation. In: Principles and techniques of electron microscopy: biological applications. 4th ed., Edinburg, UK: Cambridge University Press; (2000). pp. 4-85. DOI: 10.1006/anbo.2001.1367.
18. Suvarna K, Layton CH and Bancroft J: Immunohistochemical techniques. In: Bancroft's Theory and Practice of Histological Techniques.7th ed., Churchill Livingstone, Philadelphia; 2013. pp. 381-426.https://doi.org/10.1016/B978-0-7020-4226-3.00010-X.

19. Malatesta M: Histological and Histochemical Methods - Theory and Practice. Eur J Histochem. 2016; 60: 2639. doi: 10.4081/ejh.2016.2639.

20. Emsley R, Dunn G and White IR: Mediation and moderation of treatment effects in randomized controlled trials of complex interventions. Stat Methods Med Res. 2010; 19: 237-270. doi: 10.1177/0962280209105014.

21. Sinjari B, Feragalli B, Cornelli U, Belcaro G, Vitacolonna E, Santilli M, Rexhepi I, D'Addazio G, Zuccari F and Caputi S: Artificial Saliva in Diabetic Xerostomia (ASDIX): Double Blind Trial of Aldiamed® Versus Placebo. J Clin Med. 2020; 9: 2196. doi: 10.3390/jcm9072196

22. Kaikini AA, Dhodi D, Muke S, Peshattiwar V, Bagle S, Korde A, Sarnaik J, Kadwad V, Sachdev S and Sathaye S: Standardization of type 1 and type 2 diabetic nephropathy models in rats: Assessment and characterization of metabolic features and renal injury. J Pharm Bioallied Sci. 2020; 12: 295-307. doi: 10.4103/jpbs.JPBS_239_19

23. Smriti K, Pai KM, Ravindranath V and Pentapati KC: Role of salivary malondialdehyde in assessment of oxidative stress among diabetics. J Oral Biol Craniofac Res. 2016; 6: 41-4. doi: 10.1016/j.jobcr.2015.12.004

24. Nair A and Nair BJ: Comparative analysis of the oxidative stress and antioxidant status in type II diabetics and nondiabetics: A biochemical study. J Oral Maxillofac Pathol. 2017; 21: 394-401. doi: 10.4103/jomfp.JOMFP_56_16

25. Chen SY, Wang Y, Zhang CL and Yang ZM: Decreased basal and stimulated salivary parameters by histopathological lesions and secretory dysfunction of parotid and submandibular glands in rats with type 2 diabetes. Exp Ther Med. 2020; 19: 2707-2719. doi: 10.3892/etm.2020.8505.

26. Hassan SS and Alqahtani MS: Comparative Study of Cytokeratin Immunostaining of Parotid Gland Parenchyma in Normal, Diabetic, and Excretory Duct Ligation of Mongrel Dogs. Eur J Dent. 2023; 17: 678-686. doi: 10.1055/s-0042-1744372.

27. Chawla A, Chawla R and Jaggi S: Microvasular and macrovascular complications in diabetes mellitus: Distinct or continuum? Indian J Endocrinol Metab. 2016; 20: 546-51. doi: 10.4103/2230-8210.183480.

28. Bahroudi M, Bakhshi B, Soudi S and Najar-peerayeh S: Antibacterial and antibiofilm activity of bone marrow-derived human mesenchymal stem cells secretome against Vibrio cholerae. Microb Pathogs. 2020; 139: 103867-103883. https://doi.org/10.1016/j.micpath.2019.103867

29. Wang Y, Qi Z, Yan Z, Ji N, Yang X, Gao D, Hu L, Lv H, Zhang J and Li M: Mesenchymal Stem Cell Immunomodulation: A Novel Intervention Mechanism in Cardiovascular Disease. Front Cell Dev Biol. 2022; 9:742088-742103. https://doi.org/10.3389%2Ffcell.2021.742088

30. Song N, Scholtemeijer M and Shah K: Mesenchymal Stem Cell Immunomodulation: Mechanisms and Therapeutic Potential. Trends Pharmacol Sci. 2020; 41(9):653-664. https://doi.org/10.1016/j.tips.2020.06.009

31. Sajeesh S, Dahal S, Bastola S, Dayal S, Yau J and Ramamurthi A: Stem Cell Based Approaches to Modulate the Matrix Milieu in Vascular Disorders. Front Cardiovasc Med. 2022; 9: 879977. https://doi.org/10.3389/fcvm.2022.879977

32. Tuleta I and Frangogiannis NG: Diabetic fibrosis. Biochim Biophys Acta Mol Basis Dis. 2021;1867: 166044. doi: 10.1016/j.bbadis.2020.166044.

33. Manal MM, Ola AAM, Fatma I, Heba AH and Nadia A: Histological and Immunohistochemical Study on the Possible Ameliorating Effects of Antox on the Parotid Gland of Rats with Streptozotocin-Induced Diabetes Mellitus Type 1. Egyptian Society of Clinical Toxicology Journal. 2023; 11: 12-29. https://journals.ekb.eg/article_301590_52917df678a9332457d3bb6ef0894fb3.

34. Liu Z, Dong L, Zheng Z, Liu S, Gong S, Meng L, Xin Y and Jiang X: Mechanism, Prevention, and Treatment of Radiation-Induced Salivary Gland Injury Related to Oxidative Stress. Antioxidants (Basel). 2021; 10: 1666. doi: 10.3390/antiox10111666.

35. Domergue S, Bony C, Maumus M, Toupet K, Frouin E, Rigau V, Vozenin MC, Magalon G, Jorgensen C, Noël D. Comparison between Stromal Vascular Fraction and Adipose Mesenchymal Stem Cells in Remodeling Hypertrophic Scars. PLoS One. 2016; 11: e0156161. doi: 10.1371/journal.pone.0156161.

36. Zhou L, Xu L, Shen J, Song Q, Wu R, Ge Y, Xin H, Zhu J, Wu J and Jia R. Preischemic administration of nonexpanded adipose stromal vascular fraction attenuates acute renal ischemia/reperfusion injury and fibrosis. Stem Cells Transl Med. 2016; 5:1277-1288. doi: 10.5966/sctm. 2015-0223.

37. Vila T, Rizk AM, Sultan AS and Jabra-Rizk MA: The power of saliva: Antimicrobial and beyond. PLoS Pathog. 2019; 15: e1008058. doi: 10.1371/journal.ppat.1008058.

38. Parsons AM, Ciombor DM, Liu PY and Darling EM: Regenerative Potential and Inflammation-Induced Secretion Profile of Human Adipose-Derived Stromal Vascular Cells Are Influenced by Donor Variability and Prior Breast Cancer Diagnosis. Stem Cell Rev Rep.2018;14:546-557.doi:10.1007/s12015-018-9813-1.

39. Qian S, Wei Z, Yang W, Huang J, Yang Y, Wang J. The role of BCL-2 family proteins in regulating apoptosis and cancer therapy. Front Oncol. 2022; 12: 985363. doi: 10.3389/fonc.2022.985363.

40. You S, Zheng J, Chen Y and Huang H: Research progress on the mechanism of beta-cell apoptosis in type 2 diabetes mellitus. Front Endocrinol (Lausanne). 2022;13: 976465. doi: 10.3389/fendo.2022.976465.

41. Ceccarelli S, Pontecorvi P, Anastasiadou E, Napoli C and Marchese C: Immunomodulatory Effect of Adipose-Derived Stem Cells: The Cutting Edge of Clinical Application. Front Cell Dev Biol. 2020; 8: 236. doi: 10.3389/fcell.2020.00236.

42. Jung SY, Park DC, Kim SS and Yeo SG: Expression, Distribution and Role of Aquaporins in Various Rhinologic Conditions. Int J Mol Sci. 2020; 21: 5853. doi: 10.3390/ijms21165853.

43. Wang D, Yuan Z, Inoue N, Cho G, Shono M and Ishikawa Y: Abnormal subcellular localization of AQP5 and downregulated AQP5 protein in parotid glands of streptozotocin-induced diabetic rats. Biochim Biophys Acta. 2011;1810: 543-54. doi: 10.1016/j.bbagen.2011.01.013.

44. Jha JC, Banal C, Chow BS, Cooper ME and Jandeleit-Dahm K: Diabetes and Kidney Disease: Role of Oxidative Stress. Antioxid Redox Signal. 2016; 25: 657-684. doi: 10.1089/ars.2016.6664.

45. Lee J, Park S and Roh S: Transdifferentiation of mouse adipose-derived stromal cells into acinar cells of the submandibular gland using a co-culture system. Exp Cell Res. 2015; 334:160-72. doi: 10.1016/j.yexcr.2015.03.006.

الملخص العربى

التأثير الاصلاحى المحتمل للجزء الوعائى اللحمى على إصابة الغدة النكفية التابعة لمرض السكرى المحدث. دراسة هستولوجية في نموذج ذكر الجرذ البالغ

وفاء عبد العظيم عبده بغدادى، أسماء أحمد الشافعى، مروة محمد صبرى

قسم الهستولوجيا، كلية الطب، جامعة القاهرة، القاهرة، مصر

الخلفية والهدف من العمل: مرض السكري يؤثر سلبًا على أعضاء مختلفة، بما في ذلك الغدة النكفية. هدفت هذه الدراسة الى تقييم تأثير الجزء الوعائى اللحمى(SVF) المشتق من النسيج الدهني على اصابة الغدة النكفية في نموذج ذكر الجرذ الأبيض البالغ المصاب بالسكري.

المواد والطرق: تم تقسيم اثنان وثلاثين جرذ إلى المجموعات الاتية، المجموعة المانحة، والمجموعة الأولى (الضابطة)، والمجموعة الثانية (مصابة بالسكري ولم تعالج) حيث تم حقن الجرذان في غشاء البريتون بجرعة واحدة من ستربتوزوتوسين (STZ) ٥٠ مجم/كجم)، ثم تركت دون علاج، والمجموعة الثالثة (مصابة بالسكرى وتم معالجتها ب SVF) وقد تم معاملتها كما في المجموعة الثانية بالإضافة الى حقنة واحدة من SVF(١,٥ × ١٠٦ خلية/ جرذ) عن طريق الحقن في غشاء البريتون في اليوم السابع من حقن الستربتوزوتوسين. تم قياس وزن الغدة النكفية وعمل التحاليل الكيميائية لمستوي مالون داى الدهايد وجلوتاثيون في النسيج، وسكر الدم العشوائى، ومستوى الجلوكوز والألفا أميليز في اللعاب، ومعدل تدفق اللعاب. كما تم صبغ قطاعات من الغدة النكفية بصبغة الهيماتوكسيلين والايوسين وصبغة تلويدين الأزرق وصبغة ماسون تراى كروم وصبغة بيرايوديك شيف الحامضي والصبغ الهستوكيميائي المناعي ضد BCL-٢, AQP-٥. وأيضا تم عمل القياسات المترية الشكلية والتحليل الاحصائي.

النتائج: أظهرت النتائج الكيميائية والنسيجية تحسنًا كبيرًا في المجموعة الثالثة مقارنة بالمجموعة الثانية. فقد أدى العلاج ب SVF إلى تقليل مستويات مؤشرات الالتهاب، واستعادة نشاط الإنزيمات المضادة للأكسدة، وتحسين استقلاب الجلوكوز في الغدة النكفية. بالإضافة إلى استعادة السمات النسيجية الطبيعية لمعظم الحويصلات. على الرغم من ذلك أظهرت بعض الحويصلات بعض الخلايا ذات الانوية الداكنة المتغلظة والسيتوبلازم المفرغ واغشية قاعدية غير واضحة.

الاستنتاج: استعاد العلاج ب SVFمعظم التركيب النسيجى الطبيعى للغدة النكفية في الفئران المصابة بالسكري مشيرا إلى إمكانية استخدامه في التخفيف من الضرر الناجم عن السكري في الغدة النكفية.